ChemComm

COMMUNICATION

View Article Online
View Journal | View Issue

Cite this: *Chem. Commun.*, 2021, **57**, 7260

Received 7th June 2021,
Accepted 23rd June 2021

DOI: 10.1039/d1cc02945b

rsc.li/chemcomm

Reversible metal-centered reduction empowers a Ni-Corrin to mimic F430†

Christopher Brenig,[a] Leila Mosberger,[a] Olivier Blacque,[a] Reinhard Kissner[b] and Felix Zelder *[a]

This communication presents a novel truncated Ni^{II}-containing metbalamin and describes its reversible one electron reduction to a catalytically active Ni^{I} species, that features cofactor F430 model character. Our results strikingly demonstrate that stabilization of Ni^{I} is not restricted to the related hydroporhyrinoid ligands and is of relevance to the application of metallocorrins in (biomimetic) catalysis.

Coenzyme F430 is one of the most fascinating transition metal containing cofactors, consisting of a central Ni-ion that is embedded in a macrocyclic corphin ligand (Fig. 1A).[1–3] This special porphyrinoid complex is required by the enzyme methyl-coenzyme-M-reductase (MCR) for the last step of bacterial formation of CH_4 from CO_2.[4] In this enzymatic reaction, a thiolate (coenzyme B) and a methyl thioether (methyl-coenzyme M) are coupled to a disulfide (CoM-S-S-Co) under formation of CH_4 (Fig. 1B).[5] Different mechanisms are controversially discussed for this unusual reaction that has never been observed so far in non-enzymatic chemistry.[4,6–9] Important insights regarding the nature, coordination-, and redox chemistry of coenzyme F430 were obtained with synthetic complexes such as a Ni^{II}-tetrahydrocorphinate,[10] a Ni^{II}-tetramethylcyclam[11] or a Ni^{II}-didehydrocorrin complex embedded in a protein.[12] In this context, the structurally closest relationship with the native coenzyme reveals F430M (Fig. 1B), a pentamethylester that is semi-synthetically derived from the natural porphinoid upon dissociation from the protein.[13] Electrochemical studies with this hydrophobic model compound strikingly demonstrated one-electron reduction of the inactive Ni^{II} form to a catalytically active Ni^{I} state.[14,15]

In 2018, we reported an unprecedented chemical pathway for the synthesis of a metbalamin,[16] *i.e.* an analogue of vitamin B_{12} containing other metals than cobalt. In particular, we prepared a 5,6-dihydroxy-ni^{II}balamin derivative (**5,6-DHNibl**) in three steps starting from B_{12}, that exhibits an electronic core structure reminiscent of coenzyme F430. Recent DFT studies of Wu and Chen suggest that the Ni^{I}-form of a truncated version of our semi-artificial cofactor is enzymatically efficacious and the authors proposed superior MCR activity compared to its natural counterpart.[17] In contrast to these encouraging computational results, the redox chemistry and catalytic activity of **5,6-DHNibl** and its derivatives, as well of metbalamins in general, has not been studied so far. Inspired by seminal studies with F430M and dicyano-cobester (**DCCbs**),[18–22] the hydrophobic models of F430 and B_{12}, respectively, we report herein on the synthesis of the hydrophobic Ni^{II} corrin 5,6-dihydroxy-heptamethyl ni^{II}byrinate (**Ni-1$^+$**, Fig. 1) and its reversible one-electron reduction

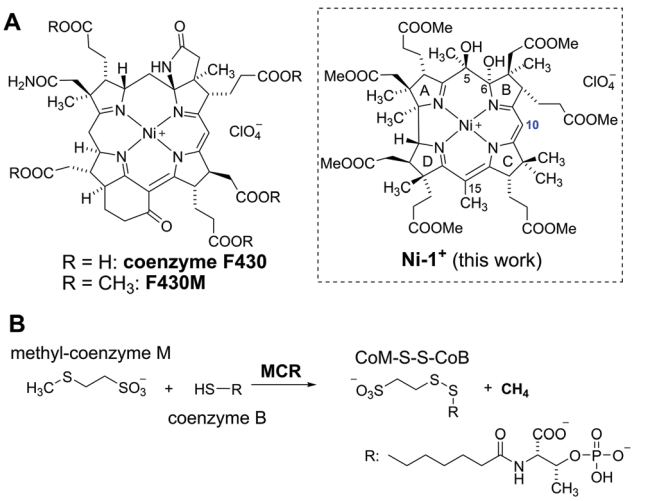

Fig. 1 (A) Structures of cofactor F430 and its hydrophobic model F430M in comparison to novel 5,6-dihydroxy-heptamethyl ni^{II}byrinate (**Ni-1$^+$**). (B) Last step of methane generation in methanogenic bacteria.

[a] *Department of Chemistry, University of Zurich, Winterthurerstrasse 190, CH-8057 Zurich, Switzerland. E-mail: felix.zelder@chem.uzh.ch; Web: www.felix-zelder.net; Fax: +41 44 635 6803*

[b] *Institute of Inorganic Chemistry, ETH Zurich, Vladimir-Prelog-Weg 1-2, 8093, Zurich, Switzerland*

† Electronic supplementary information (ESI) available. See DOI: 10.1039/d1cc02945b

Table 1 UV/Vis, cyclic voltammetry and EPR data of **Ni-1**$^+$ and **Ni-1** and their comparison to the hydrophobic cofactor F430 model **F430M**

	Ni-1$^+$		**F430M**	
	Ni^{II}	Ni^{I}	Ni^{II}	Ni^{I}
UV/Vis λ_{max} [nm] (solvent)	277, 447 (MeCN)	335, 380, 810, 880 (MeCN)	275, 440 (THF)[14]	278, 382, 754 nm (THF)[14]
CV		−0.89 (DMF, SHE)		−0.87 (DMF, SHE)[14]
$E_{1/2}$ [V] (solvent, ref.)		−0.95 (MeCN, SHE)		−1.15[a] (MeCN, Fc/Fc^+)[14]
EPR (solvent, temp)	Silent	$g_\perp$ = 1.980, $g_\parallel$ = 2.194 (MeCN, 110 K)	Silent	$g_\perp$ = 2.065, $g_\parallel$ = 2.250 (MeCN, 88 K)[14]

[a] Irreversible.

to the catalytically active Ni^I form (**Ni-1**), that shares striking key features with reduced forms of F430M (Table 1). **Ni-1**$^+$ was synthesized as perchlorate salt starting from **DCCbs**[18] in 3 steps (Scheme 1). First, 5,6-dioxo-5,6-*seco*-$Co_{\alpha\beta}$-dicyano heptamethyl cobyrinate (**5,6-DOCbs**) was synthesized from **DCCbs** according to literature.[23] Reductive demetallation of **5,6-DOCbs** with $CoCp_2$ (2.5 equiv.) and excess KCN in ^{t}BuOH led to the formation of metal-free intermediate **X** that was re-metallated without additional purification with $Ni(OAc)_2$ in MeCN under Ar(g) to the Ni^{II} complex **5,6-DONibs** in quantitative yields.

Notably, isolation of the metal-free intermediate **X** (Scheme 1) was not successful, due to its apparent high instability. Various protocols were tested to convert **5,6-DONibs** to **Ni-1**$^+$ in a subsequent ring closure reaction through pinacol-type coupling. Unexpectedly, couplings using either $CoCp_2$ or SmI_2 failed,[16,24] whereas a *McMurry* type reaction with $TiCl_4$/Zn in 1,4-dioxane finally led to **Ni-1**$^+$ in satisfactory yield (33%, isolated as **Ni-1-ClO$_4$**). Integrity of **Ni-1**$^+$ was verified by thorough spectroscopic investigations using ESI-MS (M^+, m/z_{exp}: 1069.61; M^+, m/z_{calc}: 1069.45 for $C_{52}H_{75}N_4NiO_{16}^+$), UV/Vis, as well as homo- and heteronuclear one- and two-dimensional NMR spectroscopy. Especially, ^{1}H-NMR studies underscored strikingly that **Ni-1**$^+$ with a d^8-configuration is diamagnetic and hence exhibits a square-planar coordination geometry. The UV/Vis spectrum of **Ni-1**$^+$ in MeCN displayed maxima at 263, 277, 316 and 447 nm (Fig. S3, ESI†).[25] The latter main *vis* absorption band is shifted towards longer wavelength by 7 nm compared to the *vis* absorption of **F430M**, whereas the characteristic double band at 263 and 277 nm in the UV region features higher intensity ($\varepsilon_{UV}/\varepsilon_{VIS}$ = 1.33), as it is typical for corrins.[26] This is different from the spectrum of **F430M** that exhibits a less intense single UV band at 275 nm ($\varepsilon_{UV}/\varepsilon_{VIS}$ = 0.85).[14] Overall the spectrum is similar to that of other Ni^{II}-containing corrinoids described earlier by the groups of Eschenmoser[26] and Kräutler,[27] as well as our group.[16] Analysis of the CD spectrum of **Ni-1**$^+$ indicates that the stereochemistry at C5 and C6 is identical with previously reported **5,6-DHNibl**.[16] The ^{1}H-NMR spectrum of **Ni-1**$^+$ in $CDCl_3$ revealed a singlet at 5.57 ppm for the C10 proton (Fig. 1A), thus with a strong highfield shift ($\Delta\delta$ = 0.2 ppm) compared to ring-opened *seco*corrin **5,6-DONibs**. Further details on the NMR structural elucidation of **Ni-1**$^+$ are reported in the ESI.†[25] Cyclic voltammograms of **Ni-1**$^+$ in DMF showed a distinct cathodic wave with $E_p = -(0.93 \pm 0.01)$ V *vs.* SHE (Fig. 2 and Fig. S15, ESI†) When the scan was reverted at −1.2 V, a distinct anodic wave appeared at $E_p = -(0.88 \pm 0.01)$ V with a similar peak current value as the cathodic wave. This observation, complemented by $\Delta E_p \approx 0.06$ V, is consistent with a reversible one-electron transfer redox couple. For the reversible couple, $E_{1/2}$ = −0.89 V *vs.* SHE was calculated for **Ni-1**$^+$ in DMF. A similar single reversible one-electron wave for the **Ni-1**$^+$/**Ni-1** couple was also detected in MeCN at $E_{1/2}$ = −0.95 V *vs.* SHE (Fig. S16, ESI†).[25] Reduction of the corrin ligand is unlikely to occur above −1.0 V. Free corroles, expected to be reduced more easily, are reported to undergo reduction only at

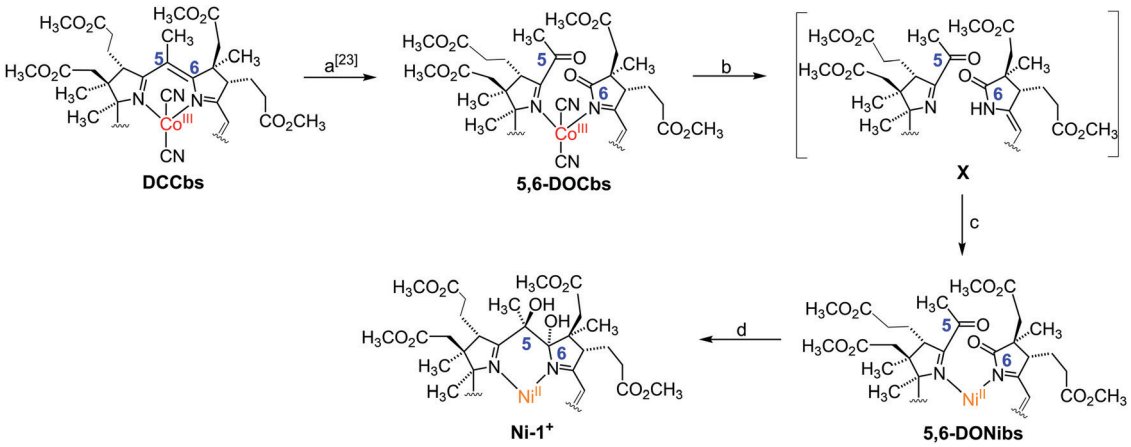

Scheme 1 Synthetic route to 5,6-dihydroxy-heptamethyl ni^{II}byrinate (**Ni-1**$^+$) starting from **DCCbs**. Only the 'northern' part of the corrin macrocycle is shown, charges and counterions were omitted for clarity. Metal-free intermediate **X** was not isolated. (a) O_2(g), methylene blue, CH_3OD, 0 °C, 7.5 h. (b) 1. $CoCp_2$ (2.5 equiv.), 2. KCN (exc.)/H_2O, ^{t}BuOH, 23 °C, 60 min. (c) $Ni(OAc)_2{\cdot}4H_2O$ (10 equiv.), MeCN (anhydr.), 23 °C, 15 min. (d) $TiCl_4$, Zn (s), pyridine, 1,4-dioxane/toluene, 1. 110 °C, 60 min, 2. 23 °C, 90 min.

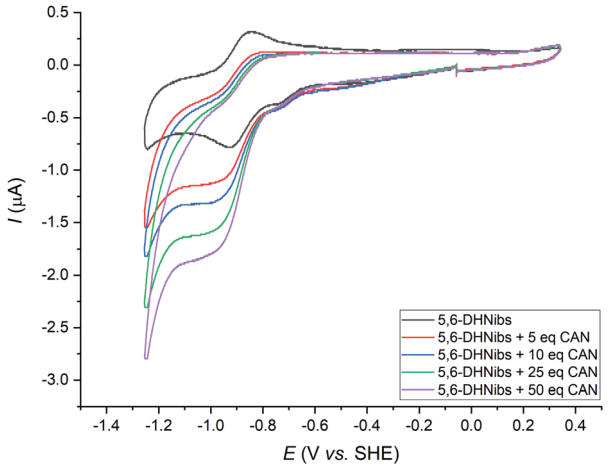

Fig. 2 Cyclic voltammograms of **Ni-1**$^+$ (0.42 mM) in DMF ([$TBAPF_6$] = 0.1 M) in absence (black trace) and presence of chloroacetonitrile (red trace: 5.0 equiv., blue trace: 10 equiv., green trace: 25 equiv. and violet trace: 50 equiv.) Scans from −0.1 V to −1.3 V to 0.3 V and back to −0.1 V at 0.1 V s^{-1}.

potentials more negative than −1.0 V.[28] Therefore, we ascribe the peak pair at −0.89 V to a Ni^{II}/Ni^{I} redox couple, similar to the one observed for **F430M** ($E_{1/2}$ = −0.87 V *vs.* SHE).[14] In a proof of principle study, we investigated the electrocatalytic reduction of alkyl halide 2-chloroacetonitrile (CAN) with electrochemically generated **Ni-1**. This reaction was extensively studied by Saveant and coworkers with Co^{I}balamins and Co^{I}-porphyrin complexes.[29,30]

Addition of CAN (5.0 equiv.) to a soln. of **Ni-1**$^+$ (0.42 mM) in DMF and subsequent cyclo-voltammetric scans allowed the detection of a catalytic current at the potential of the first reduction wave (E_p = −0.93 V *vs.* SHE) as well as a significant decrease of the absolute anodic current. With addition of increasing amounts of CAN (10–50 equiv.), the catalytic current increased notably. Furthermore, the onset potential of the catalytic reaction shifted slightly towards more positive potentials (Fig. 2). Based on these results and earlier studies with **F430M**[31] and Ni^{II}-isobacteriochlorins,[32,33] we propose reversible one-electron reduction of **Ni-1**$^+$ to **Ni-1** according to eqn (1).

$$\textbf{Ni-1}^+ + e^- \rightarrow \textbf{Ni-1} \quad (1)$$

$$\textbf{Ni-1} + NCCH_2Cl \rightarrow [NCCH_2\text{–}\textbf{Ni}^{III}\textbf{-1}]^+ + Cl^- \quad (2)$$

$$[NCCH_2\text{–}\textbf{Ni}^{III}\textbf{-1}]^+ + e^- + H^+ \rightarrow NCCH_3 + \textbf{Ni-1}^+ \quad (3)$$

It is anticipated that subsequent nucleophilic attack of **Ni-1** at the methylene carbon of CAN generates an alkylated Ni^{III} species (eqn (2)),[30] that undergoes further reduction and protonation steps to form acetonitrile ($NCCH_3$) and **Ni-1**$^+$ (eqn (3)). The latter afterwards re-enters the catalytic cycle. While this study demonstrated strikingly that electrocatalysis with **Ni-1** is principally possible, detailed electrocatalytic investigations are certainly required to unravel the underlying mechanism and the integrity of the formed product(s), as well as the scope of the biomimetic catalyst, *e.g.* its potential in the construction of C–C bonds under mild conditions.[34] The reduction process was also studied with spectroelectrochemical (SEC) methods. In an SEC cell,[25] **Ni-1**$^+$ (2.56 mM in MeCN) showed the expected, reversible reduction wave at −0.9 V (*vs.* SHE, Fig. S17, ESI†).[25] At potentials more negative than −0.6 V, changes in the absorption of **Ni-1**$^+$ are observed. The main visible absorption band at 447 nm as well absorption at 540, 316, 263 and 240 nm decreases, whereas absorption at 335 and 380 nm increases (Fig. S18, ESI†).[25] In addition to these spectroscopic changes, a pronounced strong increase in the NIR region at 810 and 880 nm is detected. These changes are consistent with the spectroscopical behavior of **F430M** upon electrochemical one-electron reduction to a Ni^{I} species for which additional electron density in the $d_{x^2-y^2}$ orbital leads to destabilization of corrin π* orbitals due to orbital mixing.[14,33] As a direct consequence more energy is required for the π → π* transitions to occur.[35] Upon reversal of the applied potential at −1.15 V, changes in absorption between 440 and 880 nm start to reverse, reaching the initial absorbance of **Ni-1**$^+$ at approx. −0.7 V on the return scan (ΔAbs = 0). The metal-centered nature of the one-electron reduction of **Ni-1**$^+$ to **Ni-1** was further corroborated by EPR spectroscopy.[25] Bulk electrolysis in MeCN allowed quantitative conversion of **Ni-1**$^+$ to **Ni-1** at −0.95 V (*vs.* Ag-wire) within 15 min, as indicated by chronoamperometry. Subsequent EPR measurements in frozen MeCN at 110 K revealed a broad, asymmetric signal with $g_\perp$ = 1.980, $g_\parallel$ = 2.194 respectively (Fig. S13, ESI†).[25] It has a p–p width of 15 mT at 110 K and resembles the spectral feature of singly reduced **F430M** at 88 K,[14] strongly supporting reduction at the metal center to a square-planar Ni^{I} species with the additional electron located in the $d_{x^2-y^2}$ orbital. Density functional theory (DFT) calculations were conducted to optimize the ground state structures of the **Ni-1**$^+$ and **Ni-1** complexes (for details see ESI†).[25] The calculations are consistent with a metal-based reduction of **Ni-1**$^+$. After reduction, the unpaired electron is mainly located on the metal center as revealed by the *Mulliken* spin density population at the Ni atom of 0.903 (Fig. 3, right). The population of one virtual frontier orbital by one electron upon reduction gives rise to a more stable structure after relaxation when it occurs on the LUMO+1 orbital (antibonding σ* between the metal $d_{x^2-y^2}$ orbital and the nitrogen p orbitals) than on the LUMO (mainly located on the tetradentate ligand with a small participation of the metal, Fig. 3, bottom right). The presence of one electron in the resultant σ orbital induces longer Ni–N bonds in **Ni-1** compared to **Ni-1**$^+$ (+0.068 Å average), but the overall geometry remains very similar with a planar $Ni–N_4$ core.

We have presented a novel truncated Ni^{II}-containing metbalamin as a suitable model of cofactor F430. Cyclovoltammetric and spectroelectrochemical studies indicate a reversible one electron reduction to a Ni^{I} species, further supported by EPR and computational investigations. A reduction potential of $E_{1/2}$ = −0.89 V *vs.* SHE was determined for the Ni^{II}/Ni^{I} couple of **Ni-1**$^+$, similar to that of F430M, a superb hydrophobic derivative of the natural Ni-containing coenzyme. In a proof-of-concept study, we demonstrated that electrocatalytic dehalogenation is principally possible with the reduced Ni^{I} corrin and intend to extend these studies to biomimetic applications and to the construction of C–C bonds under mild conditions in the near future.

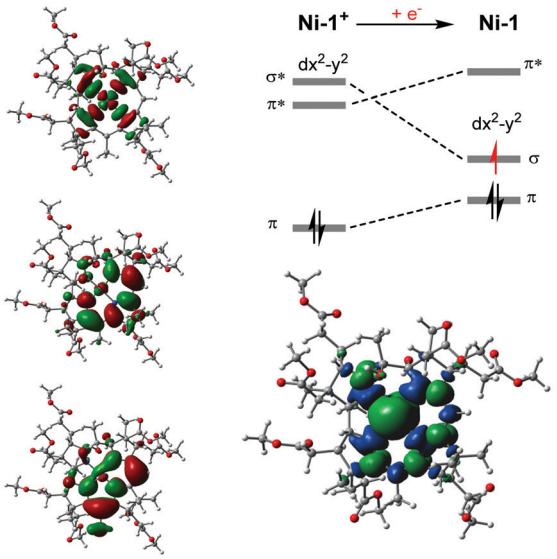

Fig. 3 Left: Plots of selected frontier orbitals of **Ni-1**$^+$; Top, right: Simplified molecular orbital diagram derived from DFT calculations; Bottom, right: Spin density plot of **Ni-1**. The newly added electron to **Ni-1**$^+$ to form **Ni-1** is highlighted in red.

F. Z. and C. B. designed the experiments and wrote the manuscript. C. B., L. M., and R. K. performed the electrochemical measurements and EPR studies. O. B. executed the computational studies.

A generous gift of vitamin B_{12} from DSM Nutritional Products AG (Basel/Switzerland) is acknowledged. We would like to thank Prof. C. Copéret (ETHZ) for access to his EPR instrument and electrochemical equipment. We are thankful to Dr. Kerstin Oppelt for help with spectroelectrochemical measurements and to Prof. P. Hamm (UZH) for provision of the SEC setup. We acknowledge preparation of synthetic precursors and measurement of IR spectra by Nicolas Yannick Nötel. This work was, in part, financially supported by the UZH 'Forschungskredit' (grant-no.: FK-17-088 to C.B.).

Conflicts of interest

There are no conflicts to declare.

References

1 A. Fässler, A. Kobelt, A. Pfaltz, A. Eschenmoser, C. Bladon, A. R. Battersby and R. K. Thauer, *Helv. Chim. Acta*, 1985, **68**, 2287–2298.
2 S. Scheller, M. Goenrich, R. Boecher, R. K. Thauer and B. Jaun, *Nature*, 2010, **465**, 606.
3 S. W. Ragsdale, *J. Biol. Chem.*, 2009, **284**, 18571–18575.
4 U. Ermler, W. Grabarse, S. Shima, M. Goubeaud and R. K. Thauer, *Science*, 1997, **278**, 1457–1462.
5 B. Kräutler and B. Jaun, in *Concepts and Models in Bioinorganic Chemistry*, ed. H.-B. Kraatz and N. Metzler-Nolte, Wiley-VCH, Weinheim, 2006.
6 R. K. Thauer, *Biochemistry*, 2019, **58**, 5198–5220.
7 S. L. Chen, M. R. A. Blomberg and P. E. M. Siegbahn, *Chem. – Eur. J.*, 2012, **18**, 6309–6315.
8 T. Wongnate, D. Sliwa, B. Ginovska, D. Smith, M. W. Wolf, N. Lehnert, S. Raugei and S. W. Ragsdale, *Science*, 2016, **352**, 953–958.
9 S. Scheller, M. Goenrich, S. Mayr, R. K. Thauer and B. Jaun, *Angew. Chem., Int. Ed.*, 2010, **49**, 8112–8115.
10 C. Kratky, A. Fässler, A. Pfaltz, B. Kräutler, B. Jaun and A. Eschenmoser, *J. Chem. Soc., Chem. Commun.*, 1984, 1368–1371.
11 M. S. Ram, C. G. Riordan, G. P. A. Yap, L. LiableSands, A. L. Rheingold, A. Marchaj and J. R. Norton, *J. Am. Chem. Soc.*, 1997, **119**, 1648–1655.
12 Y. Miyazaki, K. Oohora and T. Hayashi, *J. Organomet. Chem.*, 2019, **901**, 120945.
13 A. Pfaltz, B. Jaun, A. Fässler, A. Eschenmoser, R. Jaenchen, H. H. Gilles, G. Diekert and R. K. Thauer, *Helv. Chim. Acta*, 1982, **65**, 828–865.
14 B. Jaun and A. Pfaltz, *J. Chem. Soc., Chem. Commun.*, 1986, 1327–1329.
15 B. Jaun, *Chimia*, 1994, **48**, 50–55.
16 C. Brenig, L. Prieto, R. Oetterli and F. Zelder, *Angew. Chem., Int. Ed.*, 2018, **57**, 16308–16312.
17 J. Wu and S. L. Chen, *Chem. Commun.*, 2021, **57**, 476–479.
18 L. Werthemann, PhD thesis, ETHZ (Switzerland), Zurich, 1968.
19 H. Shimakoshi and Y. Hisaeda, *Curr. Opin. Electrochem.*, 2018, **8**, 24–30.
20 S. M. Chemaly, M. Florczak, H. Dirr and H. M. Marques, *Inorg. Chem.*, 2011, **50**, 8719–8727.
21 C. Männel-Croisé and F. Zelder, *Anal. Methods*, 2012, **4**, 2632–2634.
22 C. Männel-Croisé and F. Zelder, *Inorg. Chem.*, 2009, **48**, 1272–1274.
23 B. Kräutler, *Helv. Chim. Acta*, 1982, **65**, 1941–1948.
24 G. A. Molander and C. Kenny, *J. Org. Chem.*, 1988, **53**, 2132–2134.
25 ESI†.
26 A. Fässler, A. Pfaltz, P. Michael Müller, S. Farooq, C. Kratky, B. Kräutler and A. Eschenmoser, *Helv. Chim. Acta*, 1982, **65**, 812–827.
27 C. Kieninger, K. Wurst, M. Podewitz, M. Stanley, E. Deery, A. D. Lawrence, K. R. Liedl, M. J. Warren and B. Kräutler, *Angew. Chem., Int. Ed.*, 2020, **59**, 20129–20136.
28 J. Shen, J. Shao, Z. Ou, W. E. B. Koszarna, D. T. Gryko and K. M. Kadish, *Inorg. Chem.*, 2006, **45**, 2251–2265.
29 J. E. Argüello, C. Costentin, S. Griveau and J.-M. Savéant, *J. Am. Chem. Soc.*, 2005, **127**, 5049–5055.
30 C. Costentin, G. Passard, M. Robert and J.-M. Savéant, *Chem. Sci.*, 2013, **4**, 819–823.
31 B. Jaun and A. Pfaltz, *J. Chem. Soc., Chem. Commun.*, 1988, **4**, 293–294.
32 M. W. Renner, L. R. Furenlid, K. M. Barkigia, A. Forman, H. K. Shim, D. J. Simpson, K. M. Smith and J. Fajer, *J. Am. Chem. Soc.*, 1991, **113**, 6891–6898.
33 A. M. Stolzenberg and M. T. Stershic, *J. Am. Chem. Soc.*, 1988, **110**, 6391–6402.
34 A. Wuttig, J. S. Derrick, M. Loipersberger, A. Snider, M. Head-Gordon, C. J. Chang and F. D. Toste, *J. Am. Chem. Soc.*, 2021, **143**, 6990–7001.
35 M. W. Renner, L. R. Furenlid and A. M. Stolzenberg, *J. Am. Chem. Soc.*, 1995, **117**, 293–300.